Textures and Microstructures, Vol. 31, pp. 21–41
Reprints available directly from the publisher
Photocopying permitted by license only

INVESTIGATION OF INHOMOGENEOUS SURFACE TEXTURES WITH CONSTANT INFORMATION DEPTH: PART 1: FUNDAMENTALS

J.T. BONARSKI [a], H.J. BUNGE [b,*], L. WCISLAK [b] and K. PAWLIK [a]

[a] *Institute of Metallurgy and Materials Science, Polish Academy of Sciences, Reymonta 25, Pl-30-059 Kraków, Poland;* [b] *Department of Physical Metallurgy, Technical University of Clausthal, Grosser Bruch 23, D-38678 Clausthal-Zellerfeld, Germany*

(Received 13 May 1998)

A method is described which allows to measure pole figures under the condition of constant information depth. This is achieved by using ω- and χ-tilt simultaneously. In order to obtain satisfactory integrated intensities the use of a position sensitive detector is nearly indispensable. The functional relationship between ω and χ for constant information depth and the transformation of Euler angles $\{\varphi_1, \phi, \varphi_2\}$ to pole figure angles $\{\alpha\, \beta\}$ are given as well as the necessary intensity correction. The use of ω-tilt leads to blind areas in the centre of pole figures which can, however, be compensated by increasing the number of pole figures and using appropriate ODF programs.

The method was tested with composite samples obtained by stacking aluminium foils with known textures but with exchanging rolling and transverse direction of the uppermost foil. The results will be shown in the second part of the paper.

Keywords: Texture; Texture inhomogeneity; X-ray diffraction; Near-surface-layers; X-ray penetration depth; Constant information depth; Thin layers

INTRODUCTION

Texture analysis is mainly based on the diffraction of X-rays which have a penetration depth in most investigated materials in the order of 10–100 μm. Hence, the method actually "sees" the texture of the material

* Corresponding author.

in a layer of this order of magnitude. In many cases one is interested in the bulk texture of the material. Hence, a great number of methods have been developed on how the actually measured texture can be made representative for the bulk texture e.g. by placing the investigated layer in such a way that it cuts through different zones of the material.

On the other hand, the surface sensitivity of X-ray diffraction can also be used to study texture inhomogeneities. One way of doing that is to remove surface layers step-by-step and thus to measure texture profiles. This method is, on the one hand, cumbersome and time consuming and, on the other hand, it must still presume that the texture is homogeneous in each investigated layer (Tomov *et al.*, 1992; Tomov, 1994).

With the development of surface techniques, texture gradients have attracted great interest. Hence, methods are needed by which texture gradients can be measured non-destructively and, if possible, with a resolving power better than the penetration depth (Tarasiuk *et al.*, 1994; Tizliouine *et al.*, 1994; Chateigner *et al.*, 1994). Considerations on this line are not new. Particularly, the penetration depth can be changed by changing the wavelength of the radiation used. If synchrotron radiation is available, this allows even a continuous variation of the penetration depth. It can then be tried to deduce the texture profile from a set of measurements with (continuously) varying penetration depth.

In the conventional method of pole figure measurement in reflection technique the sample is tilted through the angle χ of the Eulerian cradle in order to obtain the pole figure values in the required range $0 \leq \alpha \leq \alpha_{max}$. Each pole figure angle α is thus measured with another sample tilt χ. Penetration of X-rays must then be considered in the diffraction plane which forms the angle χ with the sample normal direction. This leads to a different information depth from which the reflected intensity comes for each sample tilt angle. If the texture gradient to be measured is in the same order of magnitude then each angle α of the pole figure thus corresponds to another "actual" texture. Hence, the pole figure values are not consistent with each other. The same also holds for the pole figures of different $(h\,k\,l)$. If ODFs are calculated from such inconsistent pole figures the result can only be some (not very well defined) average of the texture over these varying information depths.

In order to avoid these errors, it is necessary to measure pole figures with constant information depth. This can be achieved by varying simultaneously the tilt angles χ and ω which is easily possible with

modern texture goniometers (Bonarski *et al.*, 1994; Szpunar and Blandford, 1994). On the other hand, ω-tilt is not as convenient as pure χ-tilt in as far as it requires more sophisticated techniques for measuring integrated intensities from distorted diffraction peaks and transformation of the measured intensity into pole densities required for the subsequent ODF analysis. It has, however, been shown that pole densities can be obtained even from diffraction peaks with strongly distorted profile by using a position sensitive detector. It is the purpose of the present work to develop a method of pole figure measurement and subsequent ODF analysis under the conditions of constant information depth and, eventually, to deduce the texture surface profile from measurements with different information depth.

Texture Inhomogeneity

The texture of a polycrystalline material is defined by the volume fraction of crystallites having a particular orientation g within the orientation element dg:

$$\frac{\mathrm{d}V/V}{\mathrm{d}g} = f(g); \quad g = \{\varphi_1\, \phi\, \varphi_2\}. \tag{1}$$

Strictly speaking, this definition assumes that all crystallites in the total volume V of the material are included (Bunge, 1982b).

If we cut several smaller samples out of the material we may find a different texture in each of them. One reason for that may be an insufficient grain statistics. This will, however, not be considered here. (In this case the texture will vary "erratically" with the location $\boldsymbol{r}$ at which the sample was taken.) We consider a systematic dependence of the texture on the location $\boldsymbol{r}$:

$$\frac{\mathrm{d}V/V_{\boldsymbol{r}}}{\mathrm{d}g} = f(g, \boldsymbol{r}); \quad \boldsymbol{r} = \{x_1\, x_2\, x_3\}. \tag{2}$$

Thereby $\boldsymbol{r}$ is the location of the volume $V_{\boldsymbol{r}}$ in which the texture is being considered (Fig. 1). Then $f(g, \boldsymbol{r})$ is called the *local texture* compared with the *global texture* of the material (Bunge, 1982a):

$$f(g) = \frac{1}{V}\int f(g, \boldsymbol{r})\, \mathrm{d}\boldsymbol{r}; \quad \mathrm{d}\boldsymbol{r} = \mathrm{d}x_1 \cdot \mathrm{d}x_2 \cdot \mathrm{d}x_3. \tag{3}$$

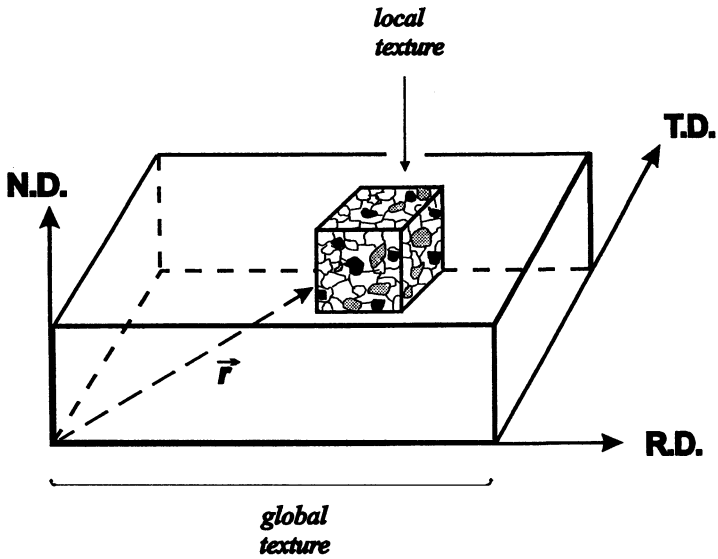

FIGURE 1 Local and global texture in a material with inhomogeneous texture.

We consider particularly the case of flat samples, the texture of which is homogeneous in the sample plane $\{x_1, x_2\}$. Inhomogeneity of the texture is only assumed in the direction x_3 i.e. the sample normal direction. Particularly, we admit that the texture may vary strongly in the vicinity of the sample surface. We further assume that we measure the texture by X-ray diffraction using a wavelength which has a penetration depth in the sample comparable with the range of strong variation of the texture. In this case the variation of penetration depth with the Bragg angle ϑ and the sample orientation angles $\{\omega\,\chi\,\varphi\}$ is superposed on the inhomogeneity of the texture. This requires that both effects be treated together.

We define pole figures as a function of the depth x_3 below the sample surface (Fig. 2):

$$P_{(hkl)}(\alpha\beta, x_3) = \frac{1}{2\pi} \oint_{(hkl)\perp\{\alpha\beta\}} f(g, x_3)\, \mathrm{d}\psi. \tag{4}$$

Thereby $\{\alpha\,\beta\}$ are the polar angles of the diffraction vector $\boldsymbol{S}$ with respect to the sample coordinate system K_A.

The beam reflected in the layer at x_3 has passed the total length $l(x_3)$ in the sample. This length is proportional to x_3 with a geometrical factor ρ

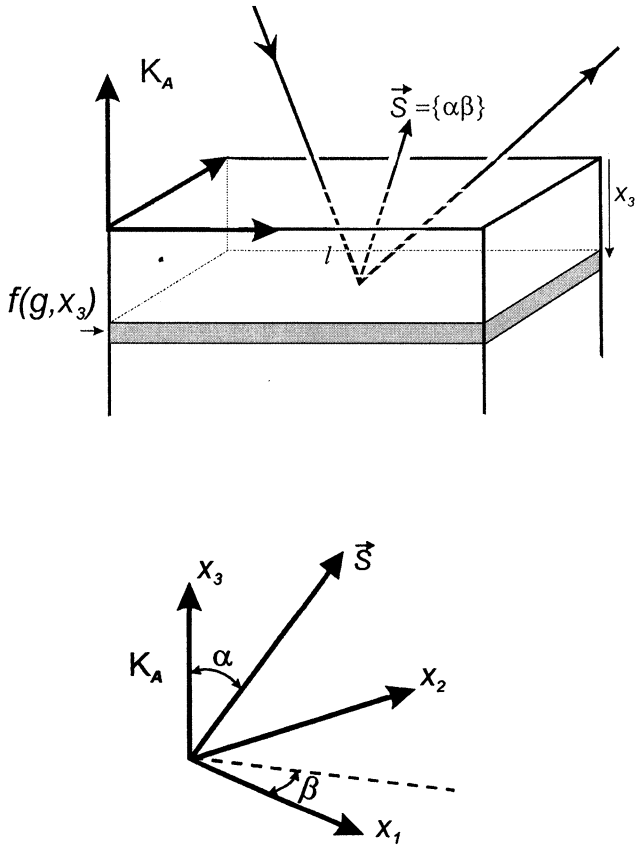

FIGURE 2 X-ray diffraction in a sample with inhomogeneous texture near the surface. Sample coordinate system K_A. The diffraction vector $\boldsymbol{S}$ defined by the incident and the reflected beam has the polar coordinates $\{\alpha\,\beta\}$ with respect to K_A. The texture in the layer parallel to the surface at the depth x_3 is $f(g, x_3)$.

depending on the goniometer angles $\{\vartheta, \omega, \chi, \varphi\}$:

$$l(x_3) = \rho(\vartheta, \omega, \chi, \varphi) \cdot x_3. \tag{5}$$

The material may have the linear absorption coefficient μ. Then the layer at x_3 contributes to the total reflected intensity by

$$\mathrm{d}I_{(hkl)}(\alpha\beta, x_3) = N_{(hkl)} \cdot F \cdot P_{(hkl)}(\alpha\beta, x_3) \cdot \mathrm{e}^{-\mu\rho x_3}\,\mathrm{d}x_3, \tag{6}$$

where $N_{(hkl)}$ is a normalization factor, F is the irradiated area on the sample surface. The total measured intensity is then given by the integral

$$I_{(hkl)}(\alpha\beta) = N_{(hkl)} \cdot F \cdot \int_0^\infty P_{(hkl)}(\alpha\beta, x_3) \cdot \mathrm{e}^{-\mu\rho x_3}\, \mathrm{d}x_3. \tag{7}$$

In the conventional pole figure measuring technique $P_{(hkl)}(\alpha\beta)$ is assumed to be independent of x_3. The integral over x_3 is then to be carried out only over the exponential term. Together with F this gives the absorption factor which is independent of the texture. If, however, $P_{(hkl)}(\alpha\beta)$ depends on x_3 then Eq. (7) can no longer be split into two independent factors.

The pole figure angles $\{\alpha\,\beta\}$ depend on the sample orientation $\{\omega\,\chi\,\varphi\}$ and if we assume a measuring technique using a position sensitive detector, then they may also depend on ϑ. Having chosen $(h\,k\,l)$, ϑ is fixed; having also chosen $\{\alpha\,\beta\}$, there is still one degree of freedom in choosing the angles $\{\omega\,\chi\,\varphi\}$. Let us assume that this can be used to keep the geometrical factor ρ independent of $(h\,k\,l)$ and $\{\alpha\,\beta\}$, then both sides of Eq. (4) can be integrated over x_3 similar to the pole figure in Eq. (7).

In order to keep the normalization conditions of pole figures and the texture function we define an averaged pole figure

$$\bar{P}_{(hkl)}(\alpha\beta) = \mu \cdot \rho \cdot \int_0^\infty P_{(hkl)}(\alpha\beta, x_3) \cdot \mathrm{e}^{-\mu\rho x_3}\, \mathrm{d}x_3, \tag{8}$$

and analogously the averaged texture

$$\bar{f}(g) = \mu \cdot \rho \cdot \int_0^\infty f(g, x_3) \cdot \mathrm{e}^{-\mu\rho x_3}\, \mathrm{d}x_3. \tag{9}$$

The factor $\mu\rho$ is the inverse of the integral over the exponential factor, and one obtains in analogy to Eq. (4)

$$\bar{P}_{(hkl)}(\alpha\beta) = \frac{1}{2\pi} \oint_{(hkl)\perp\{\alpha\beta\}} \bar{f}(g)\, \mathrm{d}\psi. \tag{10}$$

Equation (10) can be solved for $\bar{f}(g)$ in the same way as in the case of homogeneous textures with given pole figures $\bar{P}_{(hkl)}(\alpha\beta)$. Particularly

the approaches of solving Eq. (10) with incomplete pole figures are also applicable. Hence, we can expect to obtain an integrated texture according to the definition, Eq. (9) which is, however, different from the global texture defined in Eq. (3). Figure 3 illustrates schematically the influence of the exponential factor in Eq. (9) on the integral $\bar{f}(g)$. We may approximate the integral by extending it only up to the "information depth" X_ε at which the exponential factor has decreased to ε as is also illustrated in Fig. 3.

The information depth is defined (Bonarski *et al.*, 1994) by

$$X_\varepsilon = -\frac{\ln \varepsilon}{\mu \cdot \rho}, \tag{11}$$

where the value of ε defines the assumed limit for the weakest beam which is still included in the integration. The integral Eq. (9) can then be approximated by

$$\bar{f}(g) \approx \bar{f}(g)_\varepsilon = \mu \cdot \rho \cdot \int_0^{X_\varepsilon} f(g, x_3) \cdot \mathrm{e}^{-\mu\rho x_3}\, \mathrm{d}x_3. \tag{12}$$

Particularly, we shall use, later on, $\varepsilon = 0.01$. Then the neglected part of the integral is in the order of 1% which is better than the usually reached accuracy of pole figure measurement. The local texture $f(g, x_3)$ as a function of x_3 can be deduced (under certain conditions) from the averaged texture $\bar{f}(g)$ by varying the factor $\mu\rho$ i.e. the information depth X_ε from which the major part of the average comes. This can be done in two ways i.e. by varying ρ with the help of an appropriate choice of the angles $\{\omega\chi\varphi\}$ or by varying μ via different wavelengths, or by both methods together.

Texture Measurement with Constant Information Depth

In order to measure pole figures the Bragg angle ϑ_{hkl} must be chosen and the diffraction vector $\boldsymbol{S}_{hkl}$ must be brought into all required orientations $\{\alpha\beta\}$ in the sample specified in the sample coordinate system K_A (Fig. 2). For the sake of simplicity, we consider only one Bragg angle ϑ_{hkl} at a time as is shown in Fig. 4 (notwithstanding the fact that the diffraction profile of this reflection may be measured with a position sensitive detector

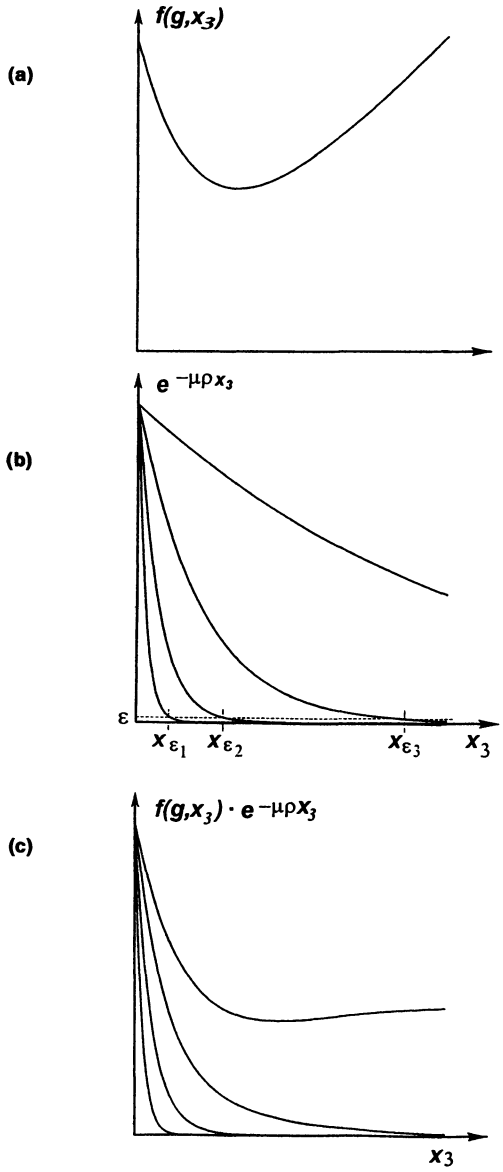

FIGURE 3 Contribution of near-surface layers to the average texture $\bar{f}(g)$, Eq. (9). (a) Depth profile of the texture $f(g, x_3)$; (b) the absorption factor as a function of x_3 for different values of $\mu\rho$. At the information depth X_ε the absorption factor has the value ε. Below that its contribution may be neglected according to Eq. (12); (c) the relative contribution of a layer at x_3 to the averaged texture defined in Eq. (9) for different values of $\mu\rho$.

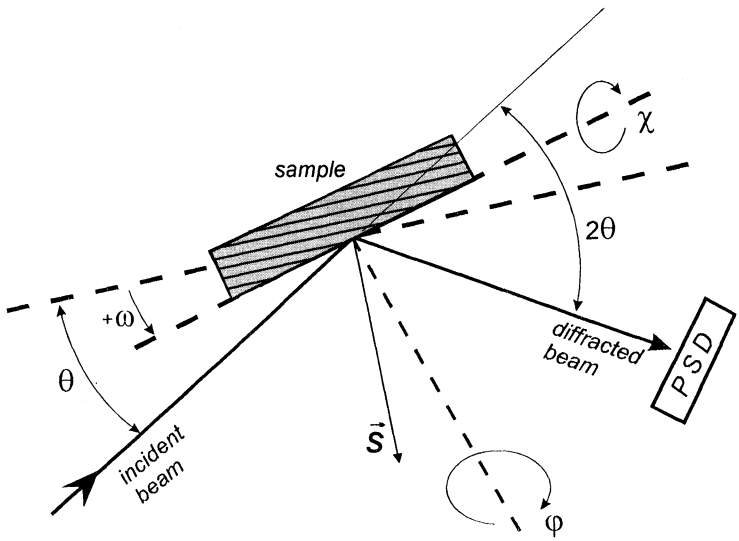

FIGURE 4 Definition of the sample angles $\{\omega\,\chi\,\varphi\}$. ω is the rotation about the goniometer axis with respect to the symmetrical Bragg–Brentano position, χ the rotation about the intersection of sample plane and reflection plane, $\chi = 0$ corresponds to the sample normal direction, and φ the rotation about the sample normal direction.

i.e. with slightly different diffraction vector for various ϑ-values within the diffraction profile). Then the orientation of the diffraction vector $\boldsymbol{S}_{hkl}$ is fixed in the goniometer. The sample must be mounted in the goniometer and must be rotated by the Eulerian cradle angles $\{\omega\,\chi\,\varphi\}$ in order to bring $\boldsymbol{S}_{hkl}$ into the position $\{\alpha\,\beta\}$.

This allows a great number of variants, of which several have been used in the literature. In the present context the following definitions are used:

- The pole figure angles $\{\alpha\,\beta\}$ are defined in Fig. 2.
- The goniometer angles $\{\omega\,\chi\,\varphi\}$ are defined in Fig. 4.

The angle ω measures a rotation of the sample about the goniometer axis, with the positive sense, towards the incident beam whereby $\omega = 0$ is the symmetric position (Bonarski *et al.*, 1994). The angle χ is a rotation about an axis in the sample plane and in the diffraction plane whereby $\chi = 0$ corresponds to the sample plane perpendicular to the diffraction plane. The angle φ is a rotation about the sample normal direction i.e. it is coaxial with the pole figure angle β. Its positive sense and origin are chosen such that $\beta = \varphi$ in the symmetrical mode i.e. $\omega = 0$.

(a) The ω–χ Relationship for Constant Information Depth

With these definitions of the goniometer angles $\{\omega\,\chi\,\varphi\}$ the geometrical factor $\rho(\vartheta_{hkl}\omega\chi\varphi)$ is given by the expression

$$\rho = \frac{\sin(\vartheta+\omega)+\sin(\vartheta-\omega)}{\sin(\vartheta+\omega)\cdot\sin(\vartheta-\omega)}\cdot\frac{1}{\cos\chi}. \tag{13}$$

It is independent of the rotation φ of the sample about its normal direction. The condition $\rho = const.$, on the one hand, defines an information depth X_ε according to Eq. (11) and, on the other hand, it fixes a functional relationship between the two sample tilt angles ω and χ (with ϑ given by $(h\,k\,l)$) according to Eq. (13) which may be written in the form

$$\omega = \omega(\chi)_{\rho=const.} \tag{14}$$

The influence of sample tilt χ in the conventional symmetrical Bragg–Brentano condition ($\omega = 0$) on the information depth $X_{0.01}$ defined according to Eq. (11) is shown as an example in Fig. 5 for the (1 1 1) reflection of Al with CoKα radiation. It is essentially the cosine function. In this condition it is $\chi = \alpha$. Hence, each circle $\alpha = const.$ of a pole figure, measured this way, would correspond to another information depth X_ε and hence to another texture average according to Eq. (12). If the texture is inhomogeneous then such a "pole figure" would not correspond to any texture at all. In fact, it would not be consistent in itself.

Combining both χ- and ω-tilt according to Eq. (13) and inserting the ρ-values in Eq. (11) gives information depths according to Fig. 6. It is immediately seen from the figure that it is now possible to move along an "equilevel" path of this profile i.e. a path of constant information depth. The curve of Fig. 5 is a one-dimensional section along $\omega = 0$ of this profile. Figure 7 shows some paths $\omega = \omega(\chi)_\rho$ according to Eq. (14) for some ρ-values.

(b) Pole Figure Coordinate Transformation

Furthermore, we need the orientation $\{\alpha\,\beta\}$ of the diffraction vector $\boldsymbol{S}$ in the sample coordinate system K_A i.e. the usual pole figure angles. They are related to the sample orientation angles $\{\omega\,\chi\,\varphi\}$ as is illustrated

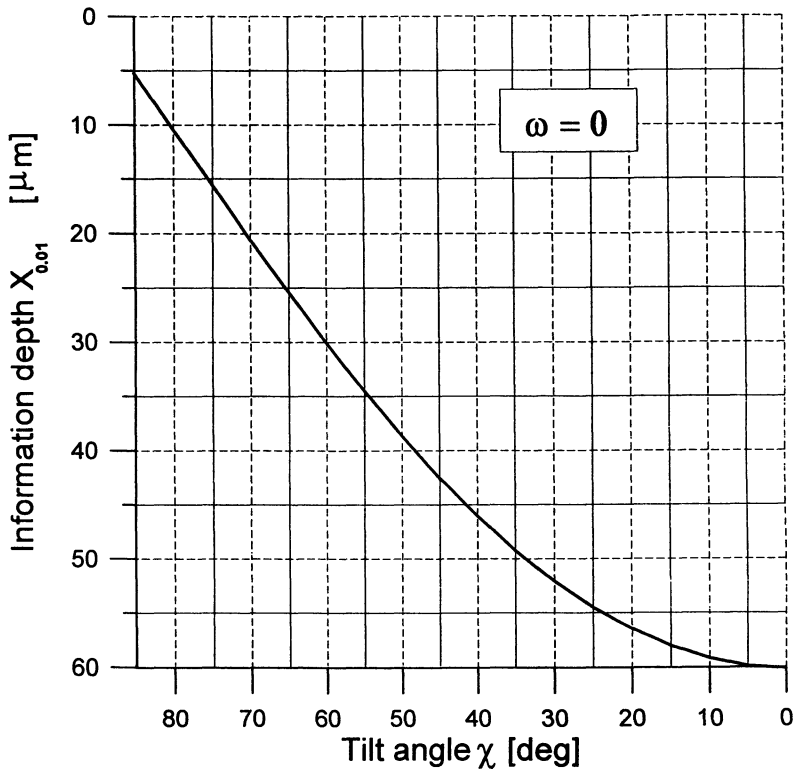

FIGURE 5 Information depth $X_{0.01}$ as a function of the sample tilt angle χ for the (1 1 1) pole figure of aluminium measured in symmetrical condition ($\omega = 0$) with CoKα radiation ($\mu = 198.1\,\mathrm{cm}^{-1}$).

in Fig. 8 with the definitions of Figs. 2 and 4. One thus obtains

$$\alpha = \arccos(\cos\chi \cdot \cos\omega), \tag{15a}$$

$$\beta_0 = \begin{cases} \arcsin(\cos\omega\ (\sin\chi/\sin\alpha)) & (\omega > 0), \\ 180^\circ - \arcsin(\cos\omega\ (\sin\chi/\sin\alpha)) & (\omega < 0), \end{cases} \tag{15b}$$

$$\beta = \beta_0 + \varphi,$$

where $-\pi/2 < \omega < +\pi/2$ and $0 \leq \chi < \pi/2$. Thereby ω is related to χ according to Eq. (14) if a measurement with constant information

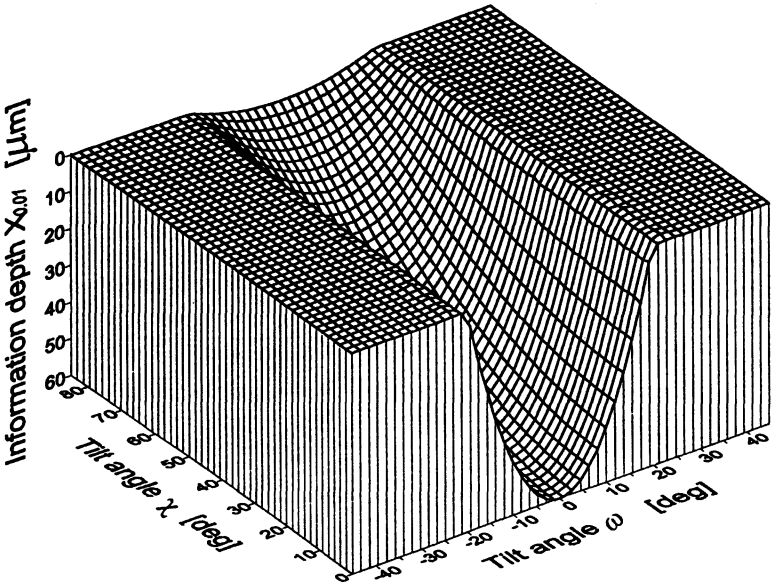

FIGURE 6 Information depth $X_{0.01}$ as a function of both tilt angles ω and χ for the (1 1 1) pole figure of aluminium with CoKα radiation ($\mu = 198.1\,\mathrm{cm}^{-1}$).

depth is considered. It is seen that the transformation relationship $\{\omega\chi\varphi\} \Rightarrow \{\alpha\beta\}$ is independent of ϑ. This is due to the definition of ω with respect to the symmetric Bragg–Brentano orientation of the sample. If a position sensitive detector is used as is indicated in Fig. 4, measuring several reflections at the same time, then this definition of ω would require another ω for each reflection. If we apply the transformation relationship (Eqs. (15a) and (15b)) to the conventional equal angular scan with respect to the goniometer angles χ and φ with $\omega = \omega(\chi)$ according to Eq. (14) then the scanning lattice $\Delta\chi, \Delta\varphi$ according to Fig. 9 (top) is "wound up" to spiral paths as is indicated in Fig. 9 (bottom). It is also seen that there is a blind area in the centre of the pole figure which cannot be measured under the condition $\rho = const.$ i.e. using the relationship $\omega = \omega(\chi)$. If this blind area is not too large, however, the ODF can still be obtained from incomplete pole figures of the type Fig. 9 (bottom) if only an appropriate ODF-calculation program is available (Bunge, 1982b; Pawlik, 1986; Dahlem-Klein *et al.*, 1993).

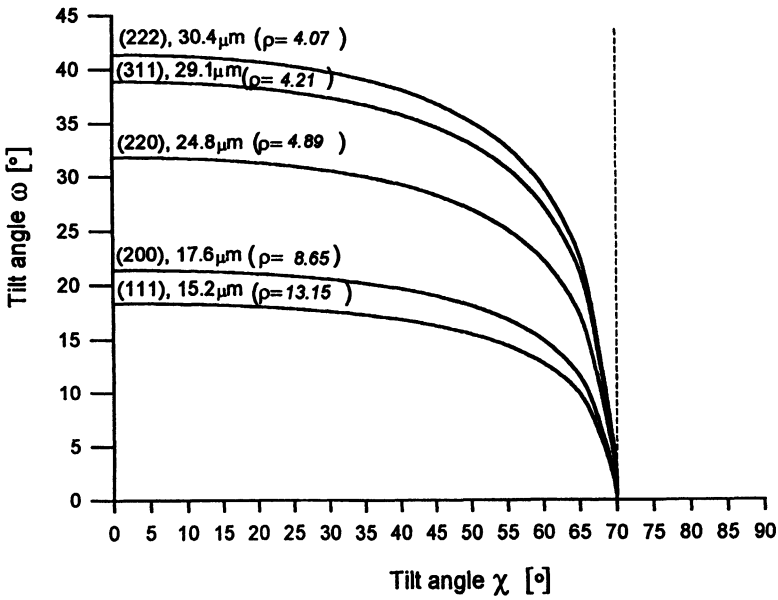

FIGURE 7 Some paths $\omega = \omega(\chi)$ for the pole figures (1 1 1), (2 0 0), (2 2 0), (3 1 1) and (2 2 2) of aluminium with constant information depth $X_{0.01} = 15.2$, 17.6, 24.8, 29.1 and 30.4 μm, corresponding to CoKα radiation. The curve for (1 1 1) is the section $X_{0.01} = 15.2$ μm in the diagram in Fig. 6.

(c) Geometrical Intensity Correction

With the definition, Eq. (8), of the averaged pole figure $\bar{P}_{(hkl)}(\alpha\beta)$ the total intensity, Eq. (7) can be written in the form

$$I_{(hkl)}(\alpha\beta) = N_{(hkl)} \cdot \frac{F}{\mu \cdot \rho} \cdot \bar{P}_{(hkl)}(\alpha\beta). \tag{16}$$

In the symmetrical Bragg–Brentano geometry the geometrical factor F/ρ is constant. Hence, in this case no intensity correction is needed *inside* the pole figure. All intensity factors (i.e. including μ) are summarized in a normalization factor which is independent of the pole figure angles $\{\alpha\,\beta\}$. The normalization factor is obtained by integrating over $\{\alpha\,\beta\}$ using the normalization condition of the pole figure. The same applies here to the factor $N_{(hkl)}/\mu$. We must, however, consider the angular dependence of the geometrical factor F/ρ.

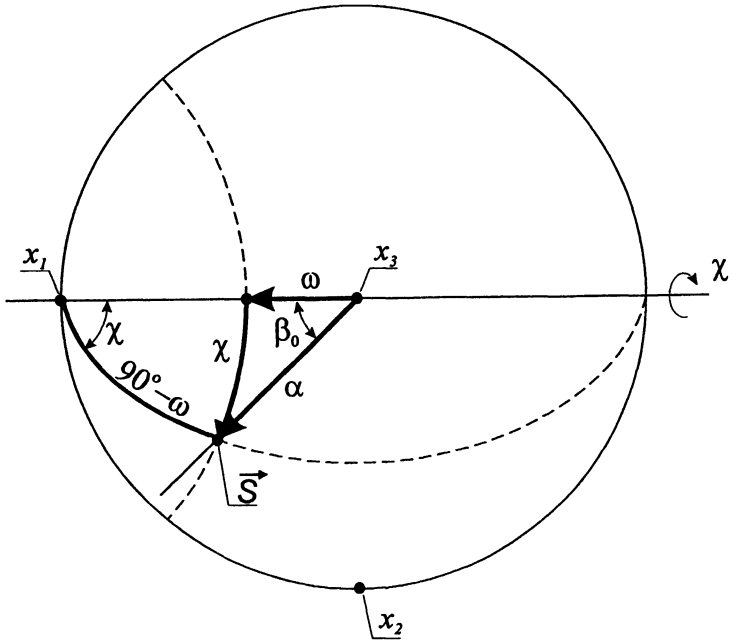

FIGURE 8 Illustrating the relationship, Eq. (15) between the Eulerian cradle angles $\{\omega\chi\varphi\}$ and the pole figure angles $\{\alpha\beta\}$. The angle β_0 corresponds to $\varphi=0$. Projection plane is the sample plane according to Fig. 4. The sample directions x_1, x_2, x_3 are defined in Fig. 2.

The irradiated area on the sample surface has the size

$$F = F_0 \cdot \frac{1}{\sin(\vartheta - \omega) \cdot \cos\chi} \tag{17}$$

(see e.g. Wasserman and Grewen, 1969), then Eq. (16) can be written as

$$I_{(hkl)}(\alpha\beta) = N_{(hkl)} \cdot \frac{F_0}{\mu} \cdot G(\vartheta, \omega) \cdot \bar{P}_{(hkl)}(\alpha\beta) \tag{18}$$

with the geometrical intensity correction factor

$$G = \frac{2 \cdot \sin(\vartheta + \omega)}{\sin(\vartheta + \omega) + \sin(\vartheta - \omega)} = 1 + \tan\omega \cdot \cot\vartheta. \tag{19}$$

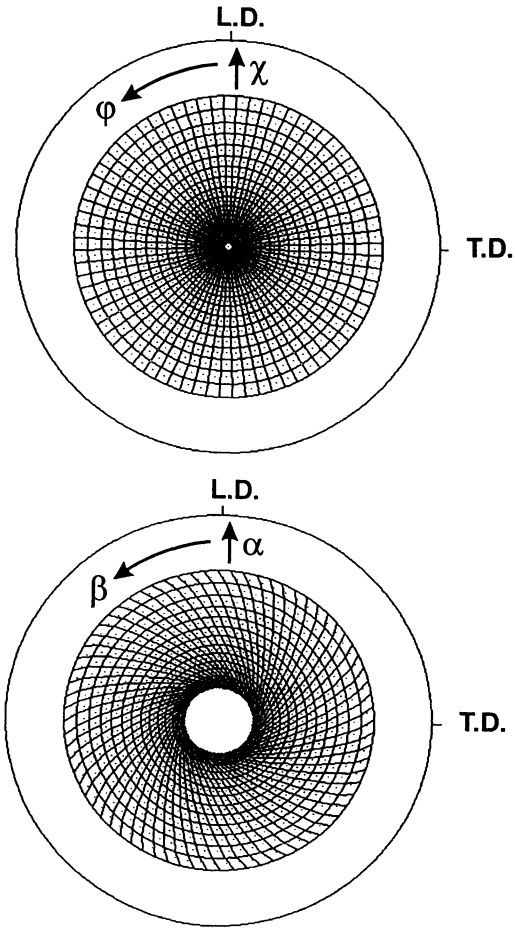

FIGURE 9 Transformation of the Eulerian cradle coordinates $\{\chi\varphi\}$ measured in equal angular steps $\{\Delta\chi\,\Delta\varphi\}$ (upper part) into pole figure angles $\{\alpha\beta\}$ (lower part) according to Eq. (15) with $\omega=\omega(\chi)$ according to Eq. (14) and $\rho=15.5°$.

For small values of ω this may be approximated by

$$G = 1 + \omega \cdot \cot\vartheta. \tag{20}$$

This relationship is shown in Fig. 10.

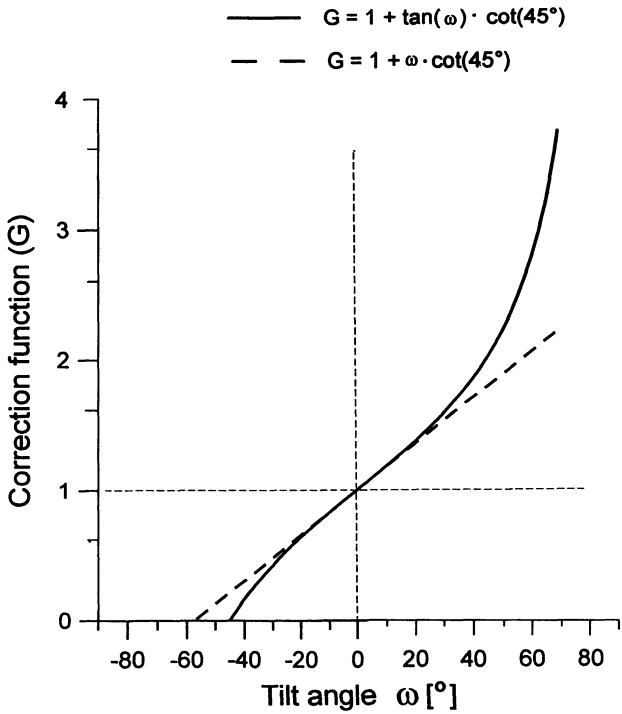

FIGURE 10 Geometrical intensity correction factor G, Eq. (19), and the approximation, Eq. (20) for $\vartheta = 45°$.

(d) Peak Distribution

The intensity $I_{(hkl)}(\alpha\beta)$ in Eq. (16) is the integral intensity of the diffraction peak measured over ϑ. The ϑ-dependence may be written in the form

$$I(\vartheta) = I^{\text{int}} \cdot b(\vartheta); \qquad \int_{\vartheta} b(\vartheta) \cdot \mathrm{d}\vartheta = 1, \tag{21}$$

where $b(\vartheta)$ is the peak shape function (Wcislak *et al.*, 1993, 1996).

In the symmetrical Bragg–Brentano condition i.e. $\omega = \chi = 0$ the focusing condition can be quite well fulfilled. In the *conventional* texture measurement only χ-tilt is being used. Thereby only one line of the

sample remains on the focusing circle, upper and lower part of the sample move inwards and outwards respectively so that symmetrical peak broadening is observed. It has been shown that in this case the peak shape function could be quite well approximated by a Gaussian distribution function

$$b_{hkl}(\vartheta) = b_{\max} \cdot \mathrm{e}^{-((\vartheta-\vartheta_0)/\sigma)^2}, \tag{22}$$

where $\vartheta_0 = \vartheta_{hkl} + \Delta\vartheta$ is the centre of the shifted peak, σ is a broadening parameter depending on the sample tilt angle χ as well as on the diffraction angle ϑ_{hkl} given by the Bragg equation

$$\lambda = 2d_{hkl} \cdot \sin \vartheta_{hkl}. \tag{23}$$

Using ω-tilt additionally to χ-tilt, broadening becomes asymmetric so that the symmetric Gauss function is no longer a good approximation. Nevertheless, in a first approximation the Gauss function can still be used as is shown in Fig. 11. The case of asymmetric conditions $\omega \neq 0$ is very sensitive to a correct sample adjustment in the goniometer as well as to the intensity distribution in the primary beam.

CONCLUSIONS

The conventional method of pole figure measurement using sample χ-tilt leads to an "information depth" X_ε which is different for different tilt angles $\chi = \alpha$. The information depths also depend on the Bragg angle ϑ_{hkl}.

If the texture is inhomogeneous in a depth comparable with the information depths the different pole figures used for ODF calculation are then no longer compatible with each other and the pole figures are even inconsistent in themselves because of the α-dependence of the information depth. Using a combination of χ- and ω-tilt, however, it is possible to obtain pole figure measurements with constant information depth. Pole figures obtained in this way correspond to an averaged texture $\bar{f}(g)$ (depending on the actually used information depth). If measurements with different information depths are combined, it is possible (under certain assumptions) to determine the depth profile of the texture.

Texture measurement with constant information depth requires a definite simultaneous tilt of the sample through ω and χ. It requires also a coordinate transformation from the goniometer angles $\{\omega\,\chi\,\varphi\}$ to the pole figure angles $\{\alpha\,\beta\}$. This transformation implies the occurrence of a

a)

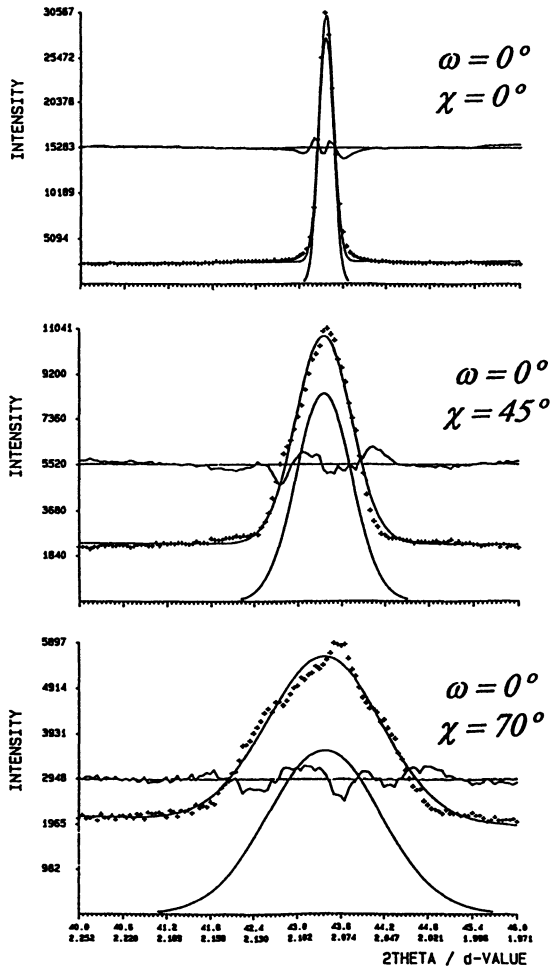

FIGURE 11(a)

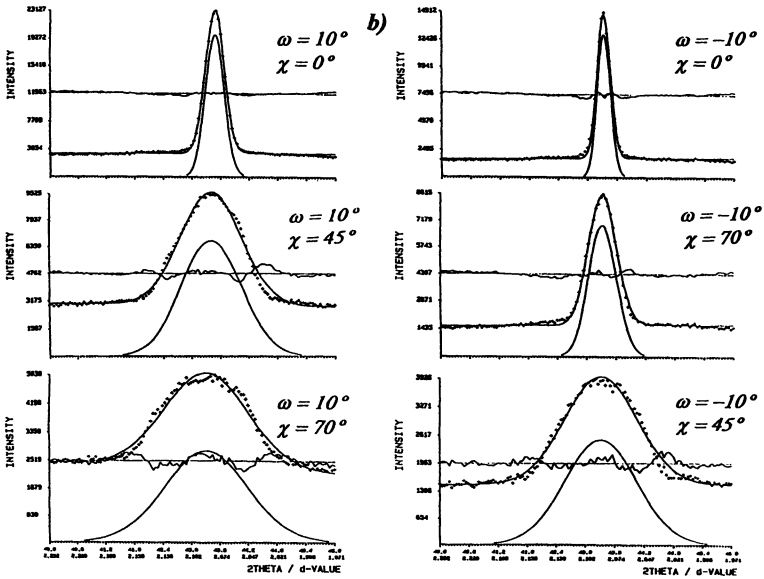

FIGURE 11(b)

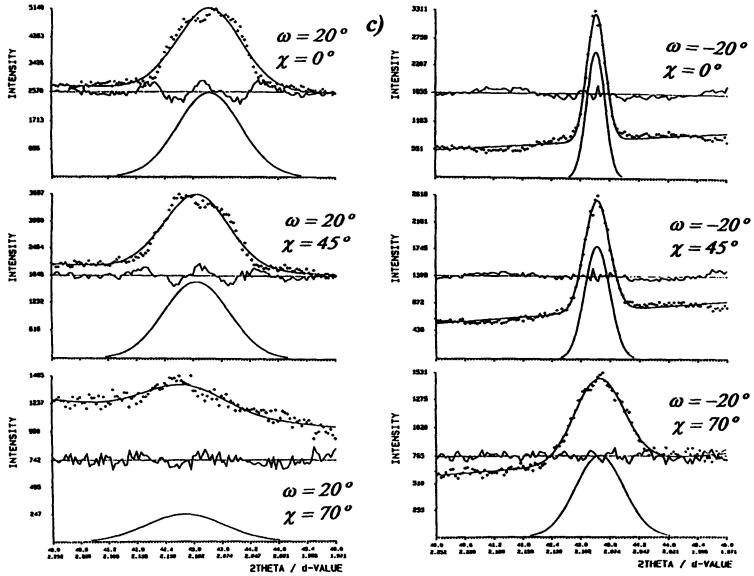

FIGURE 11(c)

FIGURE 11 Peak shapes for various sample tilt angles ω and χ as well as the approximation by Gauss profiles: (a) $\omega = 0°$ (symmetrical Bragg–Brentano geometry), (b) $\omega = -10°$ and $\omega = 10°$, (c) $\omega = -20°$ and $\omega = 20°$. The figures show the measured points and their fitting curves, the intensity profile curves (without background) and the difference curves.

blind area in the centre of the pole figures. This can, however, be compensated by using appropriate ODF programs for incomplete pole figures. Furthermore, a geometrical intensity correction is needed depending on the tilt angle ω. Finally, ω-tilt leads to much more "distorted" peak profiles than χ-tilt. It is, however, possible to "handle" such peak profiles with appropriate peak profile functions. In a first approximation, especially for small ω and χ angles, Gauss functions lead already to acceptable results. Pole figure measurement with peak profile analysis can conveniently be done with a position sensitive detector.

Acknowledgement

The authors gratefully acknowledge sponsoring of this project by the German Research Foundation DFG.

References

Bonarski, J.T., Wcislak, L. and Bunge, H.J. (1994). Investigation of inhomogeneous textures of coatings and near-surface layers. *Proc. ICOTOM-10*, Ed. H.J. Bunge, *Materials Science Forum* **157–162**, 111–117, Trans. Tech. Publ. Switzerland.

Bunge, H.J. (1982a). Inhomogene texturen. *Z. Metallkunde* **73**, 483–488.

Bunge, H.J. (1982b). *Texture Analysis in Materials Science*, Butterworths Publ. London. Second edition, Cuvillier Verlag, Göttingen (1993).

Chateigner, D., Germi, P. and Pernet, M. (1994). X-ray texture analysis in films by the reflection method. *Proc. ICOTOM-10*, Ed. H.J. Bunge, *Material Science Forum* **157–162**, 1379–1386, Trans. Tech. Publ. Switzerland.

Dahlem-Klein, E., Klein, H. and Park, N.J. (1993). ODF – Analysis for cubic crystal symmetry orthorhombic sample symmetry, *Program System*, Ed. H.J. Bunge, Cuvillier Verlag, Göttingen.

Pawlik, K. (1986). Determination of the orientation distribution function from pole figures in arbitrarily defined cells. *Phys. Stat. Sol. (b)* **134**, 477.

Szpunar, J. and Blandford, P. (1994). Equipment for texture measurement in thin films. *Proc. ICOTOM-10*, Ed. H.J. Bunge, *Materials Science Forum* **157–162**, 207–212, Trans. Tech. Publ. Switzerland.

Tarasiuk, J., Wierzbanowski, K. and Baczmański, A. (1994). Application of the method for non-destructive evaluation of texture heterogeneity. *Proc. ICOTOM-10*, Ed. H.J. Bunge, *Materials Science Forum* **157–162**, 213–220, Trans. Tech. Publ. Switzerland.

Tizliouine, A., Bessieres, J., Heizmann, J.J. and Bobo, J.F. (1994). Characterization of multilayers crystallographic texture. *Proc. ICOTOM-10*, Ed. H.J. Bunge, *Materials Science Forum* **157–162**, 227–234, Trans. Tech. Publ. Switzerland.

Tomov, I. (1994). X-ray diffraction study of texture evolution in electrodeposited zinc layers. *Proc. ICOTOM-10*, Ed. H.J. Bunge, *Materials Science Forum* **157–162**, 1495–1500, Trans. Tech. Publ. Switzerland.

Tomov, I., Banova, R. and Surnev, S. (1992). X-ray diffraction method for determination of texture evolution in layers. *Textures and Microstructures* **19**, 189–196.

Wassermann, G. and Grewen, J. (1969). *Texturen Metallischer Werkstoffe*. Springer Verlag, Berlin.

Wcislak, L., Bunge, H.J. and Nauer-Gerhardt, C.U. (1993). X-ray diffraction texture analysis with a position sensitive detector. *Z. Metallkunde* **84**, 479–493.

Wcislak, L. and Bunge, H.J. (1996). Texture analysis with a position sensitive detector. *Program System*, Ed. H.J. Bunge, Cuvillier Verlag, Göttingen.